RSC Advances

PAPER

View Article Online
View Journal | View Issue

Cite this: *RSC Adv.*, 2021, **11**, 32873

Designing hydrophobic bacterial cellulose film composites assisted by sound waves

Manolito G. Ybañez, Jr [a] and Drexel H. Camacho *[abc]

Received 14th April 2021
Accepted 24th September 2021

DOI: 10.1039/d1ra02908h

rsc.li/rsc-advances

Bacterial cellulose (BC) is a promising material for new technologies, but the range of application is limited due to its hydrophilicity. This work aims to design a hydrophobic material derived from BC, which may find use in a broad range of applications such as packaging, sensing, construction, and electronics. We report that ultrasonic treatment of BC increased the degree of material impregnation into the fiber network that altered the hydrophobic properties of the BC-based composite films. Measurements in XTM revealed that sonication enhanced the porosity of BC films from 5.77% to 22.54%. Materials such as magnesium hydroxide (MH), graphene oxide (GO), and stearic acid (SA) were impregnated into the BC films. FTIR analysis and SEM-EDS confirmed the absorption of these molecules into the BC fibers. The water contact angle (WCA) of BC films impregnated with these functional materials showed a three to four-fold increase in hydrophobicity. The incorporation of 0.3% GO in sonicated BC afforded WCA at 137.20°, which is way better than the commercial water repellant (114.90°). The sonicated BC film afforded better tensile strength and Young's modulus, up to 229.67 MPa and 6.85 GPa, respectively. This work has shown that ultrasonic treatment improved the absorption capability of BC towards hydrophobic functionalization.

Introduction

Cellulose is the most abundant renewable biopolymer resource available. It has been used in various applications because it exhibits good mechanical, thermal, and acoustic insulation properties. It is lightweight, non-abrasive, poses no health hazards, is biodegradable, and exhibits CO_2 neutrality making it an eco-friendly material.[1] Cellulose is mainly produced from plants but certain species of bacteria, algae, and fungi can also make cellulose.[2] Specifically, bacterial strains from the genera Acetobacter, Rhizobium, Agrobacterium, and Sarcina can synthesize cellulose. The cellulose they produce is called bacterial cellulose (BC), which was first described in 1886.[3] BC is pure cellulose without the hemicellulose and lignin impurities common in plant-derived cellulose.[4–6] Currently, the large-scale production of BC utilizes the Gram-negative aerobic Acetobacter strains (also known as Gluconacetobacter) under a static immersed cultivation setup.[2] During the BC synthesis, glucose chains are formed inside the bacteria, which they extrude out through their tiny pores. The glucose chains then associate to form nano-sized fibers that aggregate into ribbons forming a 3-D web-shaped micro-fiber network with hollow spaces in between creating a material with extended surface area and highly porous medium.[7] As such, BC exhibits unique properties that are generally superior to plant-derived cellulose: it is pure, has a higher degree of crystallinity, higher water capacity,[8] and exhibits Young's modulus comparable to that of aluminum.[9] Hence, BC is an excellent material worth exploring for new applications.

Despite their unique properties, BC and cellulosic materials in general, fail in the area of hydrophobicity limiting their use in many potential industrial applications. Cellulose is inherently hydrophilic and the capacity of cellulose for water absorption is unusually high due to the numerous hydrophilic hydroxyl moieties. Consequently, its mechanical properties degrade significantly as the cellulose crystals and fibers become distorted in the presence of water.[10,11] Thus, there is a need to develop a cellulosic material that is hydrophobic yet capitalizing on the advantageous properties of cellulose. Several attempts were reported to improve the water resistance of BC by means of incorporating hydrophobic agents. For instance, enhanced hydrophobicity of BC using beeswax films improved Water Contact Angle (WCA) measurements as high as 124°.[12] Similarly, natural biopolymer zein was utilized to improve BC's WCA up to 110.5°, which shows versatility of BC in developing new materials.[13] It is the hypothesis of this work that the incorporation of hydrophobic moieties can control and improve the hydrophobicity of cellulose. Moreover, this work surmises that ultrasonic treatment of BC increases the degree of material impregnation into the fiber network. This work highlights the simple method

[a]*Chemistry Department, De La Salle University, 2401 Taft, Avenue, Manila 0922, Philippines. E-mail: drexel.camacho@dlsu.edu.ph*

[b]*Central Instrumentation Facility, De La Salle University, Laguna Campus, LTI Spine Road, Barangays Biñan and Malamig, Biñan City, Laguna 4024, Philippines*

[c]*Organic Materials and Interfaces Unit, CENSER, De La Salle University, 2401 Taft Avenue, Manila 0922, Philippines*

of fabricating thin-film composites from BC by pre-treating it with sonic waves to make it more porous and impregnating it with different components to control and improve the film's hydrophobic properties.

Experimental

Materials

Fresh bacterial cellulose (BC) hydrogel sheets (250 × 150 × 20 mm) were obtained from a small-scale industry in Malvar, Batangas, Philippines that manufactures *nata de coco*, a popular delicacy prepared using a proprietary mixture of glucose, acetic acid, and coconut water with *Gluconacetobacter xylinus* under static fermentation method. Analytical grade H_2O_2, H_2SO_4, and $KMnO_4$ were purchased from Qualikems Fine Chem Pvt. Ltd. Analytical grade stearic acid ($C_{17}H_{35}CO_2H$), graphite powder, $Mg(OH)_2$, NaOH, HCl, and ethanol were purchased from Sigma Aldrich. All chemicals were used as received without further purification.

Purification of bacterial cellulose

The wet BC pellicles harvested from the air/liquid interface medium as a white jelly material were soaked in distilled water for 2 days and washed repeatedly to remove the remaining ingredients. The residual bacteria were removed by boiling (~95 °C) the BC pellicles in 1% (w/v) sodium hydroxide solution for 60 min.[14] After purification, the BC hydrogels were rinsed with distilled water until neutral pH and further stored in distilled water at 4 °C.

Ultrasonication of bacterial cellulose

The wet BC pellicles cut in 10 × 5 cm^2 were all sonicated in an ultrasonic bath (frequency: 53 kHz; output power: 500 W) for 2 h unless otherwise specified. The treatment was carried out in an ice/water bath maintaining the temperature below room temperature. Another batch of BC was first dried under oven condition (40 °C for 16 h), followed by sonication. The sonicated BC samples were then oven-dried for 16 h at 40 °C unless otherwise specified.

Preparation of impregnating solutions/suspensions

Magnesium hydroxide (MH) powders (3.0, 5.0, and 10.0 g) were dissolved in separate 100 mL methanol solutions to prepare 3, 5, and 10% solutions, respectively. To obtain uniform dispersion of particles, the solutions were treated ultrasonically to disintegrate the large agglomerates with an output power of 500 W for 30 min in an ice bath. Graphene oxide (GO) was first prepared by oxidation of graphite powder using a modified Hummer's method.[15] Graphite powder (8.23 g) and $NaNO_3$ (8.24 g) were stirred in 210 mL 98% H_2SO_4 for 2 h in a 1000 mL volumetric flask kept at an ice bath (0–5 °C) with continuous stirring. $KMnO_4$ (20.15 g) was gradually added to the solution while keeping the temperature less than 15 °C. The mixture was then stirred at 35 °C for 18.0 h. The resulting solution was diluted by adding 400 mL of water under vigorous stirring and heated up to 98 °C. The suspension was treated by adding 40 mL of 30% H_2O_2 solution and 150 mL of distilled water. The resulting graphite oxide suspension was washed by repeated centrifugation, first with 5% HCl aqueous solution and then with distilled water until the pH neutrality. The GO nanostructures were obtained by adding 160 mL of water to the resulting precipitate and further sonicated for 1 h to attain a uniform suspension of GO. The resulting solution was then dried for 48 h at 60 °C to remove the moisture. Different solutions containing 0.1, 0.2, and 0.3% w/w of GO were prepared in separate containers using water as the solvent following the recommended concentration range for a workable GO suspension with minimal agglomeration.[16,17] Stearic acid (SA) (1.0, 2.0, and 3.0 g) was dissolved in different containers containing 100 mL of 98% ethanol solution for impregnation to form 1, 2, and 3% solutions, respectively.

Impregnation and preparation of BC composites

Two protocols of BC impregnation were compared: impregnation in wet sonicated BC (referred to herein as S-W) and impregnation in dried sonicated BC (referred to herein as S-D). The sonicated (S) wet (W) or dry (D) BC were immersed separately in 200 mL of varying concentrations of MH, GO, and SA solutions/suspensions for 24 h at 60 °C. The composite films were washed thoroughly using excess distilled water to remove any excess reagents on the membrane surface. The washed impregnated BC pellicles were then oven-dried for 12 hours at 50 °C. Non-sonicated (NS) BC samples were also prepared as a control to compare the effects of sonication in the incorporation of these compounds. The varying protocols and corresponding codes (Fig. 1) of the fabricated BC composites are henceforth used: non-sonicated wet BC (NS-W), sonicated wet BC (S-W), non-sonicated dry BC (NS-D), and sonicated dry BC (S-D). The impregnated substance codes are likewise added in the corresponding composite BCs where XX could either be magnesium hydroxide (MH), graphene oxide (GO), stearic acid (SA), or the commercial hydrophobic agent NeverWet™ (NW™).

Characterization of the composite film

Fourier-transform infrared (FTIR) with an Attenuated Total Reflectance (ATR) attachment (Agilent Cary 630 FTIR/ATR

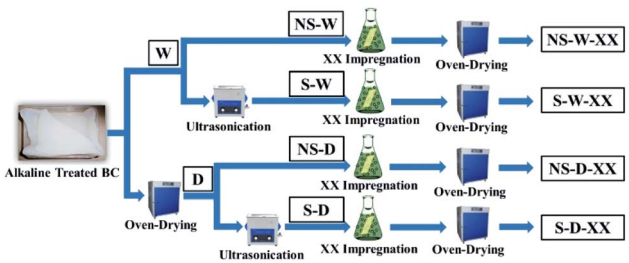

Fig. 1 Labelling of fabricated BC. (W = wet; D = dry; NS = non-sonicated; S = sonicated; XX = could either be magnesium hydroxide (MH), graphene oxide (GO), stearic acid (SA), or the commercial hydrophobic agent NeverWet™ (NW™)).

system G8044A A) was used to collect detailed information of the functional groups on the surface of the prepared BC composite films and control samples. All spectra were recorded with an accumulation of 45 scans and a resolution of 4 cm^{-1} in a range of 4000 to 650 cm^{-1}. The morphology of BC films was evaluated using Field Emission Scanning Electron Microscope (FE-SEM) imaging coupled with an Energy Dispersive X-ray Spectroscopy (EDS) detection system for atomic inspection and elemental identification (JEOL InTouchScope™ series JSM-IT500). The dried samples were analyzed using 10.00 kV acceleration voltage and ×20 000 magnification. SEM images were performed using a low vacuum to avoid surface charging. The X-ray Imaging and Microtomography experiment was performed using synchrotron radiation X-ray tomographic microscopy (SRXTM) technique with scan angle 160.0 to −20.9° with 2.4 tesla multipole wiggler (MPW) source (SLRI, Thailand).

The tensile strength of the films was tested with a universal testing machine (Zwick/Roell Z0.5) at a constant crosshead speed of 50 mm min^{-1} and a load cell of 0.5 kN. Five (5) replicates of the 150 × 15 mm^2 (l × w) samples with average film thickness in the range of 0.04–0.08 mm were conditioned at 25 ± 1 °C with 40 ± 1% humidity for at least 40 h. The specimens were loaded using a grip separation of 50 mm and proceeded with extension using the parameters until the specimen's breakage.

WCA in triplicates were performed according to ASTM C272-16 where a drop of distilled water was placed on three (3) 75 mm × 75 mm sample surface and the contact angles were measured using ImageJ Image Processing and Analysis Software contact angle measuring system. The Water Holding Capacity (WHC) of BC pellicles were investigated in different ultrasonication time treatments. The initial, post-sonication (wet state), and post-drying (dried state) mass of BC samples were recorded to show the influence of ultrasonication. The WHC measurements were measured to describe the BC's capacity to hold water while in its original wet state. Conversely, Water Absorbing Capacity (WAC) measurements were recorded to determine the capacity of BC film in dried state to absorb water. The two have similar formula but WHC describes BC in wet state while WAC describes BC in dry film state. The WHC gives insight of the inherent capacity of BC to hold such large amount of water with respect to its dried fiber weight. The WAC, on the other hand, provides information on the capacity of BC to absorb material (*e.g.*, water) after its drying process. The WAC of the samples was measured by the sieve-shake method. The dried BC sample sheets were immersed in distilled water for 12 h to completely swell up the samples. The sheets were then taken out of the storage container using tweezers. The samples were put in a sieve and were quickly shaken twice to remove the surface water and weighed. The samples were allowed to dry at ambient temperature. Samples were dried at 40 °C for 24 h to completely remove the water. The WAC and WHC of the different samples were calculated using the following formula:[18]

$$\text{Water absorbing capacity (WAC)} = \frac{\text{mass of water absorbed during soaking (g)}}{\text{dry weight of BC sample (g)}}$$

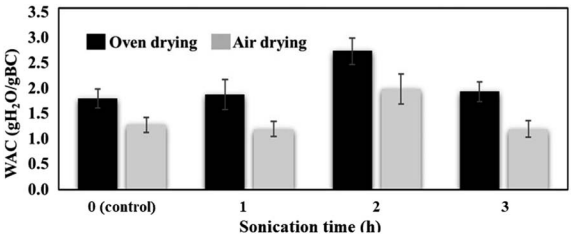

Fig. 2 Water absorbing capacities (WAC) of wet BC sonicated (S-W) at different times and drying conditions after ultrasonic treatment.

$$\text{Water holding capacity (WHC)} = \frac{\text{initial mass (g)} - \text{post drying mass (g)}}{\text{dry weight of BC sample (g)}}$$

Statistical analysis

Triplicate data of WAC, WHC, and WCA and five (5) replicates for tensile test were collected. Each data was subjected to two-way and one-way analysis of variance (ANOVA), and significant differences between means ($P < 0.05$) were determined by Duncan's Multiple Range Test (DMRT).

Results and discussion

Effects of ultrasonication on the bacterial cellulose

Water easily absorbs in cellulose films interacting with the many hydroxyl groups in cellulose through H-bonding. The water absorption capacity (WAC) of a material determines its utility involving water applications. When a cellulosic material has a high WAC value, it absorbs a lot of water, which limits its practicality as the mechanical strength decreases. However, the high WAC value of cellulosic material is indicative of its ability to absorb and store functional compounds within its fibrous network. The enhancement of the WAC of BC material was explored in this work using the ultrasonic treatment. Ultrasound provides pressure variations at solid/liquid interfaces that promote enhancement of mass transfer and increases the rate of water absorption along with the functional compounds dissolved in it. This effect was attributed to the ultrasonic waves that create rapid series of alternating contractions and expansions (sponge effect) of the material, which generates microscopic channels accelerating the rates of water absorption.[19] The results of the ultrasonic treatment of BC (Fig. 2) revealed that the sonication process increased the WAC of the BC films significantly ($p < 0.05$) revealing a high 52.57–55.20% increase in WAC obtained at 2 h sonication time. The results agree with the swelling observation by Song *et al.*[20] where the ultrasonicated BCs significantly increased the WAC up to 1.5 times higher compared to non-sonicated samples. Similarly, a study by Abral *et al.*[21] revealed that addition of sonicated cellulose to a composite sample increased the moisture absorption capacity of the material. The difference in the WAC of these BC samples can be associated with their unique porosity brought by

ultrasonic treatment. The effect of sonic waves in the BC samples is attributed to the cavitation phenomena[22] where the water molecules are absorbed and trapped physically on the surface and inside the BC membrane consisting of reticulated fibrils.[23] The empty spaces among the BC fibrils instituted more water penetration and adsorption onto the fiber matrix.[24] At longer sonication treatment (*i.e.* 3 h), the WAC decreased, which suggests that the BC fibers suffered a structural collapse that deteriorated their capacity to hold more water than shorter time ultrasound treatments. The method of drying also affected the WAC (Fig. 2) showing higher absorption capacities when the wet sonicated BC samples were dried using uniform temperature inside the oven compared to the room-temperature air-drying process where it interacts readily with moisture.

BC has a unique capability to hold high amount of water within its polymer network. Interestingly, BC is water-insoluble and due to its large network of fibers, it has a very large surface area.[8] BC can hold water up to 200 times its dry mass because of its unique nano-morphology and its ability to form extensive hydrogen bonds that allows efficient interaction with water.[8] In this current work, the water holding capacity (WHC) of wet BC pellicles treated at different sonication times were compared. The initial, post-sonication (wet state), and post-drying (dried state) masses of BC samples were recorded to show the influence of ultrasonication (Table 1) ($p < 0.05$). Results show that sonication induced mass loss of 27.02% to the wet BC upon 2 h ultrasonic treatment affording a high 98.71% WHC, which is significantly higher than the non-sonicated sample. This loss of mass was attributed to the sound energy introduced by ultrasonication that yields acoustic cavitation (*i.e.*, development, evolution, and breakdown of bubbles in the membranes)[25] promoting gradual collapse of air gaps and shock waves on the surfaces of BC fibers that subsequently cause scission and disintegration.[26] This observation was associated with the prolonged ultrasonication, which results in depolymerization leading to molecular weight reduction.[27] To illustrate the influence of sonication in the porosity and absorption of materials (MH, GO, and SA), the X-ray tomographic images of sonicated and non-sonicated BC films revealed that sonication treatment enhanced the porosity of the BC film from 5.77% to 22.54% (Fig. 3A) which is critical in the process of material impregnation. More porous materials facilitate the incorporation of guest molecules. XTM images of impregnated films showed that sonicated BC films exhibit rougher surfaces compared to the non-sonicated films indicative of better incorporation of molecules into films treated with sonic waves. Thickness measurements of sonicated and non-sonicated BCs after the impregnation process generally showed that sonicated BC films prepared using different concentrations have greater thickness compared to the non-sonicated control samples suggesting that greater impregnation of molecules were observed after sonication (Fig. 3B′–D′).

Characterization of the composite BC films

SEM of the raw non-sonicated wet BC sample (NS-W raw) shows the fibrous cellulose (Fig. 4A). Upon sonication, the fibrous network in the S-W raw sample showed a more porous surface

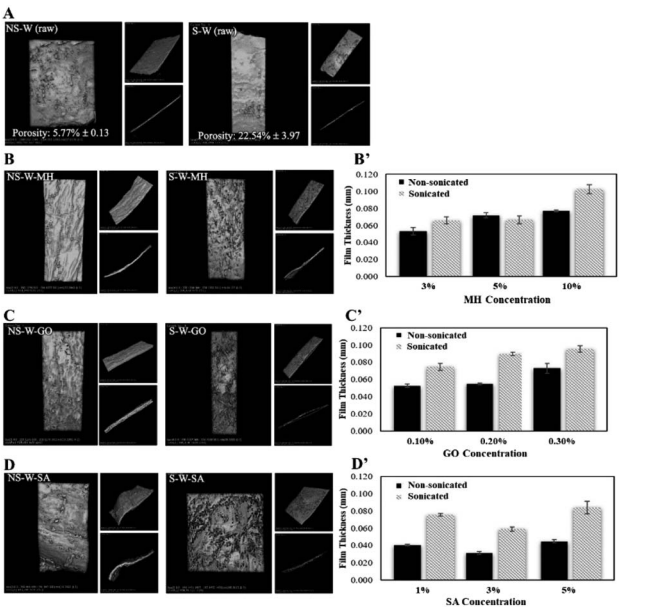

Fig. 3 XTM images of the non-sonicated (NS-W, left) and sonicated (S-W, right) bacterial cellulose (BC) films: (A) raw BC; impregnated with (B) magnesium hydroxide (MH); (C) graphene oxide (GO); and (D) stearic acid (SA). Thickness of dried BC films at different concentrations of impregnating solutions: (B′) magnesium hydroxide (MH); (C′) graphene oxide (GO); and (D′) stearic acid (SA).

Table 1 Water holding capacity of wet BC sonicated at different times

Sample	Sonication time	Initial mass (g)	Post sonication mass (g)	% Mass loss[a]	Post drying mass[b] (g)	% Mass loss[c]	Water holding capacity[d] (%)
NS-W (control)	0	110.27 ± 0.25	—	—	1.97 ± 0.06	109.30	98.22*
S-W-1 h	1	173.43 ± 0.40	137.00 ± 0.20	21.00	2.17 ± 0.06	135.83	98.75**
S-W-2 h	2	167.40 ± 0.26	122.17 ± 0.21	27.02	2.17 ± 0.06	76.94	98.71**
S-W-3 h	3	158.23 ± 0.67	117.66 ± 0.20	25.64	1.87 ± 0.06	37.00	98.03***

[a] % Mass loss with respect to its initial mass. [b] Post-drying mass using oven drying technique. [c] Mass loss with respect to its post sonication mass. [d] Data obtained from triplicate experiments and is presented as mean ± S.D. Any two average values in the same column followed by the same number of asterisks are not significantly different ($p < 0.05$).

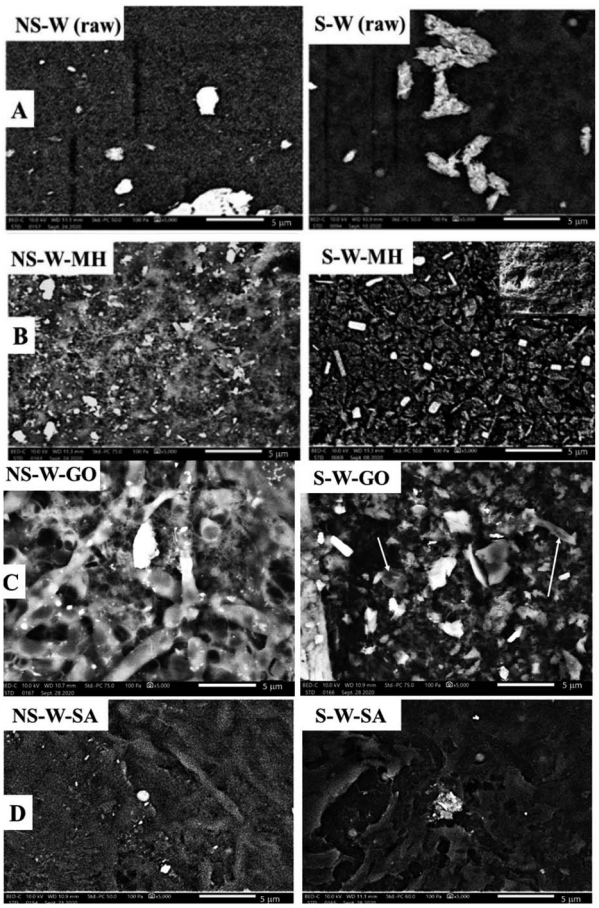

Fig. 4 SEM images of the non-sonicated wet (NS-W, left) & sonicated wet (S-W, right) bacterial cellulose (BC) films: (A) raw; (B) impregnated with 10% magnesium hydroxide (MH); (C) impregnated with 0.3% graphene oxide (GO), white arrow represents GO sheet; (D) impregnated with 3% stearic acid (SA).

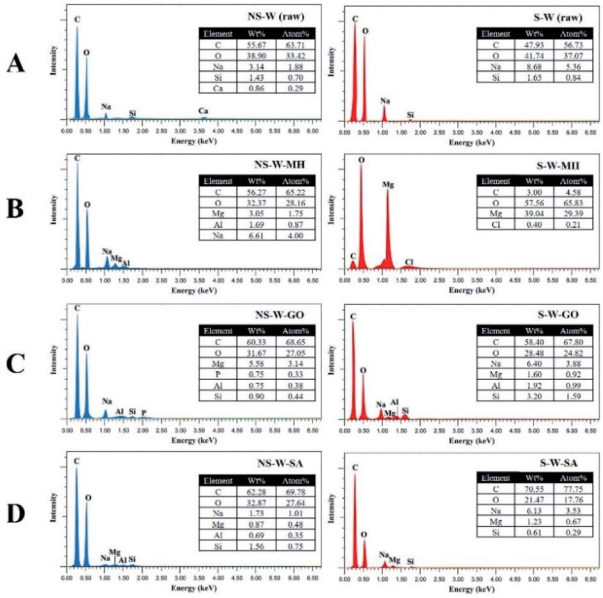

Fig. 5 EDS of the non-sonicated (NS-W, left) and sonicated (S-W, right) bacterial cellulose (BC) films: (A) raw BC; (B) impregnated with 10% magnesium hydroxide (MH); (C) impregnated with 0.3% graphene oxide (GO); and (D) impregnated with 3% stearic acid (SA).

consistent with the XTM observation. The ultrasonic treatment of BC induced swelling and disintegration of the cellulose fibers, which increased its porosity. Notable differences in the morphologies of impregnated BC films are observed comparing the non-sonicated from the sonicated composite films (Fig. 4B–D). Fig. 4C showed the characteristic GO sheet incorporated in the matrix. GO fillers are completely unified in the cellulose composite as reported by Han *et al.*[16] The energy dispersive X-ray spectroscopy (EDS) analysis (Fig. 5) showed the difference in elemental composition for sonicated and non-sonicated BC films. The presence of Mg atoms in MH-impregnated BC films indicates the impregnation of Mg where more Mg atoms were observed in S-W-MH (29.39% atom) compared to the NS-W-MH (1.75% atom) sample suggesting that ultrasonication increased the absorption of MH into the BC fibers. The presence of GO and SA, however, cannot be confirmed by EDS since they both contain carbon and oxygen but the morphologies of the sonicated composites are notably different (Fig. 4C and D).

The FTIR spectra of the raw BC and composite films impregnated with various functional materials (Fig. 6) showed that impregnation afforded chemical modifications in the BC structure. The major peaks of raw BC film at 3345, 2900, 1300, 1050 cm^{-1} established the purity of the cellulose.[28] The distinguished peak of 3345 cm^{-1} and shouldering around 3300 cm^{-1} to 3500 cm^{-1} indicate O–H stretching, wavenumbers 2800 cm^{-1} to 2900 cm^{-1} signify C–H stretching, 1160 cm^{-1} shows C–O–C stretching and 1035 cm^{-1} to 1060 cm^{-1} correspond to C–O stretching (Fig. 6A). The spectra of NS-W (raw) and S-W (raw) are broadly similar, which indicates no significant effect on the chemical structure of BC. However, ultrasonication and impregnation caused few shifting of the wave numbers and/or % transmittance of the main BC spectra peaks. For instance, sonicated BC spectra showed more intense peaks characteristic of impregnated materials, which indicate greater amounts have been incorporated into the BC. The FTIR spectra of the $Mg(OH)_2$-impregnated BC (Fig. 6B; S-W-MH) showed a strong peak at 3696 cm^{-1} assigned to the OH stretching with the influence of divalent metal forming the M^{2+}–OH bond[29] and is related to the degree of hydrogen bonding among neighboring OH groups.[30] The peak, which is brought about by the Mg^{2+}–OH interaction in cellulose, confirms that $Mg(OH)_2$ is well absorbed in the sonicated BC film than in the non-sonicated sample. The functional groups of the GO-impregnated BC (Fig. 6C) showed three peaks, centered at 3343, 1718, and 1626 cm^{-1} correlated to the stretching vibrations of O–H, C=O, and C=C bonds, respectively.[31] Moreover, the peak at 1535 cm^{-1} appeared upon the incorporation of GO in the BC, which indicates a strong interaction (hydrogen bonding) between BC and GO, causing a downshift of the GO C=O group band indicative of more GO interacting with BC chains.[32] The functional group present in SA was shown by peaks at 2840 cm^{-1} and 2910 cm^{-1}, which are assigned to the stretching vibrations of $-CH_2$ groups.[33] The

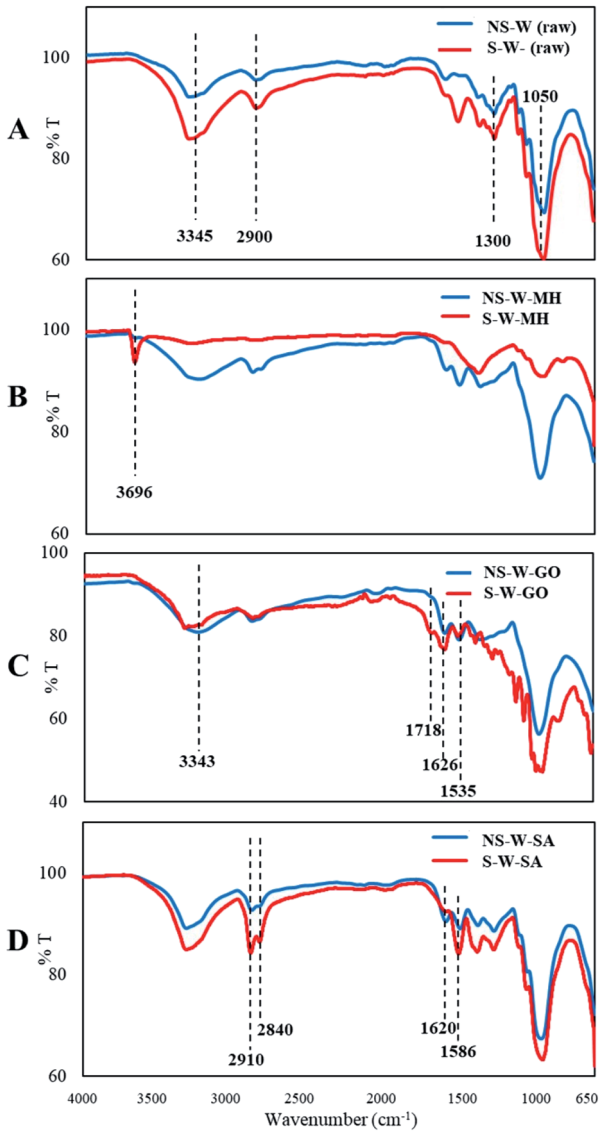

Fig. 6 FTIR spectra comparison of non-sonicated wet (NS-W) and sonicated wet (S-W) bacterial (BC) composite films impregnated with: (A) raw BC; (B) 10% magnesium hydroxide (MH), (C) 0.3% graphene oxide (GO), and (D) 3% stearic acid (SA).

intense IR band at 1620 cm^{-1} corresponded to the COO^- stretching mode of SA (Fig. 6D). The absence of the typical C=O stretch for the stearic acid in SA-impregnated BC was ascribed to its interaction with the cellulose chains. The disappearance of the carbonyl stretching at 1706 cm^{-1}) of SA has also been observed by Zeng *et al.* as SA reacts with the other substrates in the composite.[34] This is supported by the appearance of peak at 1586 cm^{-1} which is attributed to the asymmetric and symmetric stretches of the $-COO^-$ group.[35]

Water contact angle (WCA) measurements

BC fibers contain numerous hydroxyl groups responsible for their hydrophilic nature. When a water droplet interacts with the hydrophilic BC films, the WCA on the surface is <90° indicative of the water spreading over the surface. Typically, the WCA of cellulose films is in the range of 17° to 47°.[36,37] In this current work, the raw BC films were recorded to have contact angles at 33.50° and 30.20° for non-sonicated and sonicated wet BC, respectively. Conversely, if WCA is >90°, the surface tends to avoid the spreading of water, which is an indication of a hydrophobic surface. The impregnation of hydrophobic materials into the BC fibers alters the hydrophilicity of BC films. Specifically, different concentrations of MH, GO, and SA suspensions were used to investigate their interaction with BC in improving the hydrophobicity (Fig. 7). Results show that the WCA measurements of non-sonicated wet (NS-W) BC films impregnated with MH (Fig. 7A) remain the same despite increasing the concentration of MH. Upon sonic pre-treatment, the WCA increased from 57.40° at 3% MH to 106.90° and 106.80° at 5 and 10% MH soaking concentrations, respectively, a three-fold increase in WCA compared to the control. The composite BC films above the horizontal line at WCA 90° separates the surfaces with hydrophobic properties. Using GO, significant increases in WCA were observed when the BC is pre-treated ultrasonically (Fig. 7B). Impregnation of 0.1, 0.2, and 0.3% GO suspensions on sonicated wet BC increased the WCA of the composite film to 60.40°, 133.20°, and 137.20°, respectively. The threshold angle of >90° for hydrophobicity indicates that incorporation of 0.3% GO imparted the highest hydrophobic property, a four-fold increase in hydrophobicity compared to the control. The S-W-SA composite films similarly showed a notable 3.5-fold increase in WCA at 99.80°, 117.70°, and 108.60° for 1, 2, and 3% SA, respectively (Fig. 7C). The improved hydrophobicity of the cellulose films after the treatment using MH can be attributed to the reduced number of

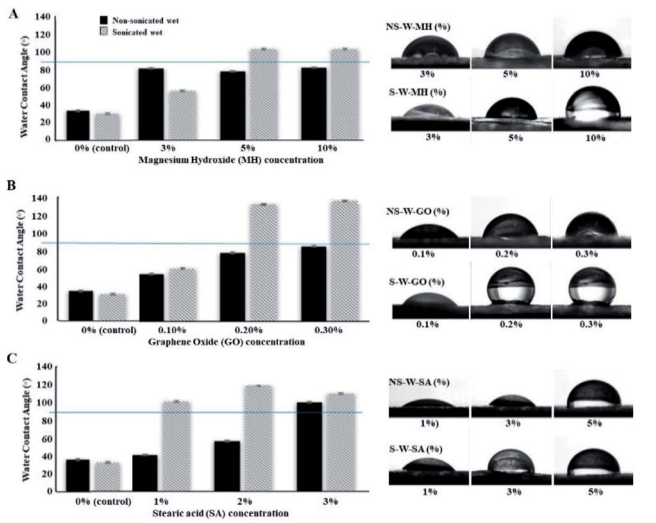

Fig. 7 Water contact angle (WCA) measurements of water droplet on the surface of non-sonicated wet (NS-W) and sonicated wet (S-W) bacterial cellulose (BC) films impregnated with different concentrations of (A) magnesium hydroxide (MH); (B) graphene oxide (GO), and (C) stearic acid (SA). Composite BC films above the horizontal line at WCA 90° separates the surfaces with hydrophobic properties. Insets: WCA images of a water droplet on the indicated BC composite surface.

accessible hydroxyls on the bacterial cellulose (BC) surface, which leads to a limited interaction with water. Moreover, MH is sparingly soluble in water (0.00122 g/100 mL), which also afforded hydrophobic property in BC. Its incorporation into the BC structure *via* electrostatic interaction with the cellulose hydroxyl groups reduces the BC's ability to accommodate water molecules. In support to this, the appearance of strong peak at 3696 cm^{-1} has been assigned to the OH stretching with the influence of the M^{2+}–OH bond. Similar observation was reported by Khanjani *et al.* where divalent metals interacted with the cellulose.[38] Further, Dong *et al.* presented a molecular model for the interaction between divalent metal cations and carboxylate groups from two adjacent chains on one cellulose fibril.[39] GO is generally amphiphilic brought by the nonpolar hydrophobic moieties of nanosheets and the polar hydrophilic regions from oxygenated defects.[40] GO imparts hydrophobic character arising from its two-dimensional structure and existence of sp^2-bonded carbon atoms. In the same manner, SA being a non-polar long-chained hydrocarbon also imparted a high degree of hydrophobicity as the chain entangles into the network of cellulose fibers. Hydrophobization of BC was successfully achieved where the amounts of impregnated substances increased as the BC is pre-treated ultrasonically, which is consistent with the increased water absorption capacity allowing the easy mass transfer into the network of cellulosic fibers.

Generally, wet BC films pre-treated with sonic waves (S-W) then impregnated with the functional materials displayed superior water repellency over the non-sonicated wet (NS-W) BC (Fig. 8A and B). On the other hand, using dried BC before ultrasonic pre-treatment showed inferior ability to absorb the functional materials as evidenced by the <90° WAC (Fig. 8C and D). To compare with a reference material, a commercially available NeverWet™ water-repellent additive (NW™) was used to prepare the positive (+)-control BC films (Fig. 8F and G).

The reference material reportedly contains the hydrophobic yet flammable naphtha (petroleum), heavy aromatics, and mineral spirit components. Incorporation of NW™ in NS-W and S-W BC films afforded WCA results at 100.50° and 114.90°, respectively, confirming that sonic pre-treatment increased the impregnation of the hydrophobic materials. Comparison of the different pre-treatment and impregnation protocols (Fig. 8H) shows that the S-W-GO composite BC film afforded superior hydrophobic property, which is better than the (+)-control commercial hydrophobization agent. The result is associated with the amphiphilic property of GO brought by its nonpolar hydrophobic moieties of the nanosheets and the polar hydrophilic regions from oxygenated defects.[40] Despite the not-so-hydrophobic nature of MH and SA, hydrophobicity was still observed. As one reviewer pointed out, the roughness-induced hydrophobicity on the surface can contribute to the observation. The presence of Mg ions and long entangling chains of SA induces roughness on the BC surface, which affects the wetting properties leading to hydrophobic response.[41]

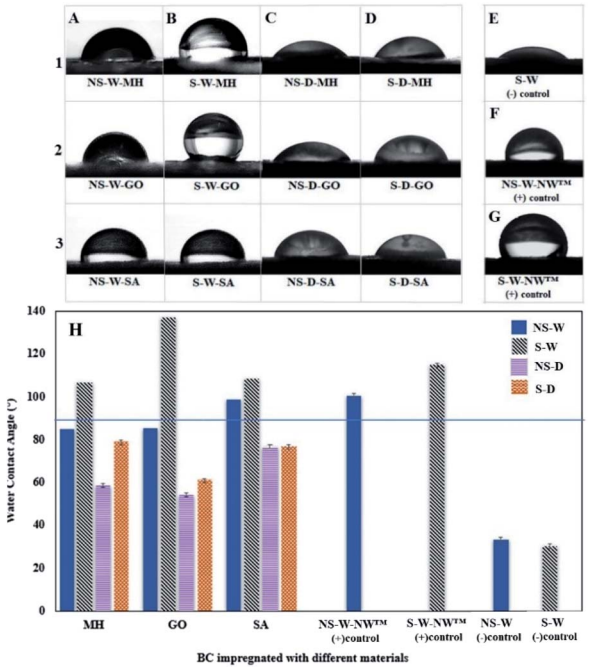

Fig. 8 Water Contact Angle (WCA) images of a water droplet on the surface of a (A) non-sonicated wet (NS-W), (B) sonicated wet (S-W), (C) non-sonicated dry (NS-D), and (D) sonicated dry (S-D) bacterial cellulose (BC) films impregnated with (1) magnesium hydroxide (MH), (2) graphene oxide (GO), and (3) stearic acid (SA); WCA images on the (E) raw sonicated wet (S-W) BC as (–) control, (F) non-sonicated wet (NS-W) and (G) sonicated wet (S-W) BC impregnated with commercial NeverWet™ (NW™) water-repelling product as (+) controls; (H) bar graph of the WCA measurements of differently processed BC films impregnated with different materials. Composite BC films above the horizontal line at WCA 90° separates the surfaces with hydrophobic properties. All samples were prepared using the best concentration as determined in Fig. 7.

Mechanical properties of composite BC films impregnated with functional materials

The mechanical properties of a material are key factors in many applications as it defines the disintegration of molecules upon application of force.[42] The typical tensile strength (force at breaking point), elongation at break point, and Young's modulus of unmodified BC films are in the range 28–200 MPa, 2–6%, and 2–13 GPa, respectively. The variation depends on factors, such as culture conditions, drying conditions, and bacteria strain used during the production of the BC.[43–46]

The stress–strain curves for the BC composite films (Fig. 9A) and the averaged measured data obtained from tensile testing of the samples (Fig. 9B) show that the raw film prepared by sonicating BC (S-W raw) afforded the highest averaged tensile strength and Young's modulus values reaching up to 229.67 MPa and 6.85 GPa, respectively, which are way better than the films prepared from commercially available cellulosic products, which are all standard plant-based celluloses (STD1 and STD2). The superior mechanical property is attributed to the network of cellulose in the formation of pellicles during its biosynthesis, which resulted in an improved alignment in the 3D structure of the BC fibers. In comparison to non-sonicated BC (NS-W raw), the enhanced mechanical properties of

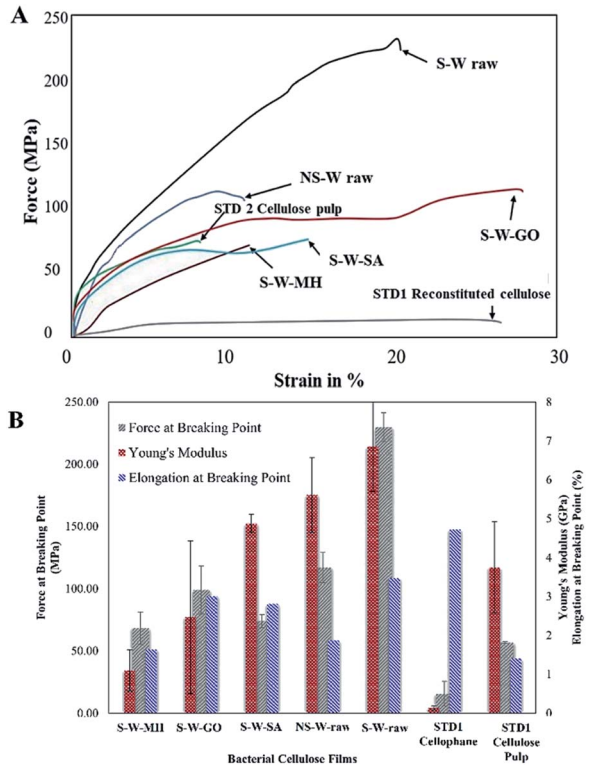

Fig. 9 (A) Stress–strain curve of sonicated BC composite films, (B) mechanical properties of sonicated BC composite films.

sonicated BC (S-W raw) can be related to its improved orientation which, makes BC fibers tighter. It has been discussed in literature that ultrasound treatment has been shown to facilitate the formation of more compact and tight film and thus improve its moisture resistance.[47,48] Several studies reported that sonication afforded a tightly-arranged microstructure brought by the improved interweaving and bonding within the fiber, which remarkably decreased the defects and ultimately improved the mechanical strength of cellulose structure.[46,49] Therefore, improved structure from molecular to macroscopic scale contributes to the overall excellent mechanical properties of BC films. The tensile strength significantly increased in two folds upon ultrasonic treatment of BC as compared with the non-sonicated BC (117.25 MPa) ($p < 0.05$). While the standard Cellophane® (reconstituted cellulose, STD1) film recorded the highest elongation at breaking point, the BC films have generally stronger tensile strength and elasticity. These data confirm that BC films are mechanically strong materials that are promising in the field of materials science. Comparison between the impregnated BC films shows that the impregnation of -MH, -GO, and -SA into the BC, showed reduced tensile strength indicative of weaker interactions. Similar trends in the mechanical properties of the BC were observed in the literature upon the incorporation of molecules into the BC network.[45] With the impregnation of BC, the fabricated films showed reduced toleration towards the applied stress during the tension test. When compared with that of the pure BC film, the tensile strength and Young's modulus of the impregnated BC films were found to be approximately 30–75% and 15–35% lower, respectively. This observation could be explained by the disruption of the hydrogen bonding between BC fibrils due to the addition of interfering compounds, which resulted in the decrease in mechanical properties of the films.[50] In comparison with the mechanical properties of BC composites reported in literature, modified BC exhibited lower tensile strength and Young's modulus, at 2–31 MPa, 0.13–0.26 GPa, respectively, while the elongation at breaking point (8–28%) (Table 2) showed the polymeric composites to be more flexible. The incorporation of several molecules decreased the mechanical strength of the BC. This observation can be linked with the reduced available H-bonding in the BC network. To address this, addition of a binding agent such as crosslinkers can be used to improve the tensile strength.

Insights on the utility of hydrophobic cellulose

Hydrophobic cellulose materials are of interest for niche applications such as specialty papers that repel water in preserving important documents. The material platform of bacterial cellulose makes the production of specialty paper a sustainable process. The added step of sonication and incorporation of functional materials is simple and practical, which can easily be incorporated in large scale production. Hydrophobic papers prevent the absorption of moisture, which can be utilized in designing packaging materials for products that are sensitive to moisture. Hydrophobic packaging materials prevent the entry of moisture preserving the integrity of the product thus eliminating the need for desiccants. These desiccants pose hazard as these can accidentally be eaten by unsuspecting consumers such as small children. The hydrophobic cellulose can also be utilized as a substrate or base

Table 2 Comparison of mechanical properties of BC with other works

BC film composite	Force at breaking point (MPa)	Young's modulus (GPa)	Elongation at breaking point (%)
BC-MH[a]	68.20 ± 13.07	1.70 ± 0.71	1.63 ± 0.47
BC-GO[a]	98.90 ± 19.48	1.70 ± 4.70	3.00 ± 0.91
BC-SA[a]	73.97 ± 5.35	5.00 ± 5.00	2.81 ± 0.38
BC-chitosan[51]	10.26 ± 1.52	0.132 ± 0.46	28.54 ± 7.76
BC-starch[52]	31.06 ± 0.89	0.361 ± 0.19	5.3 ± 0.10
BC-SA/CM[b,53]	2.33 ± 0.03	0.250 ± 0.05	8.24

[a] BC composite films in this work. [b] Sodium alginate/carboxymethylated BC.

material in sensing applications where water or moisture interferes with the sensing mechanism. New materials can be designed maximizing the advantages of the cellulose and exploiting this hydrophobization technique for the fabrication of smart materials that are responsive to external stimuli. Films of this hydrophobic cellulose can potentially be used as a membrane in separation technologies preventing moisture or water from passing through. The incorporation of GO in hydrophobic paper can further be exploited to maximize the unique properties of GO in improving the conductive and optical properties of the cellulose.

Conclusions

The applications of bacterial cellulose (BC) are limited due to the inherent hydrophilic property. The 2 h ultrasonic treatment increased the porosity of BC, which significantly influenced the water absorption capacity (WAC) up to 1.5 times higher compared to non-sonicated samples indicating a higher tendency to incorporate functional materials within the BC fiber network. Ultrasonic treatment effectively facilitated the successful impregnation of functional molecules (magnesium hydroxide (MH), graphene oxide (GO), and stearic acid (SA)) into the BC pellicles. Changes in the SEM morphologies, the EDS detection of Mg, and the characteristic absorbances in FTIR confirmed the absorption of these molecules into the sonicated BC fibers. The mechanical testing showed the improvement in tensile strength of the BC film upon sonication but the presence of functional molecules in between the fiber network of the composite films weakened the material upon application of force. The high amounts of impregnated molecules in ultrasonically-treated BC resulted in hydrophobization of the BC composite films where significant increases in water contact angle (WCA) were observed upon impregnation of MH, GO, and SA in sonicated BC. The incorporation of 10% MH afforded a three-fold increase in WCA compared to the control. The impregnation of 0.3% GO in sonicated wet BC films recorded a notable four-fold WCA increase (137.20°) while a 3.5-fold of increase in WCA (108.60°) was observed for incorporating 3% SA. The use of GO in composite BC film afforded superior hydrophobic property, which is better than the (+)-control commercial water-repelling agent. This study has shown that ultrasonic treatment has dramatically improved the absorption capability of BC, which resulted in the improvement of its hydrophobicity. By improving the water-resistance of BC, more applications can be explored increasing the utility of this sustainable cellulosic material. Further investigations utilizing other molecules of interest are recommended to incorporate different functionalities to the BC films. The leaching of the impregnating material out of the BC composite and its impact on the physical property are worth investigating.

Author contributions

Manolito G. Ybañez Jr: conceptualization, methodology, investigation, formal analysis, writing – original draft. Drexel H. Camacho: conceptualization, methodology, resources, supervision, writing – reviewing and editing.

Conflicts of interest

There are no conflicts to declare.

Acknowledgements

This research did not receive any specific grant from funding agencies in the public, commercial, or not-for-profit sectors. The Philippine Nuclear Research Institute (PNRI) Chemistry Research Section, and the De La Salle University - Central Instrumentation Facility (DLSU-CIF) spectroscopy and electron microscopy laboratories are acknowledged for the use of instruments. We wish to acknowledge Alona Intac, Cristian Ryan Argamino, and Dr Jose Esmeria, Jr of DLSU-CIF for assistance in conducting the instrumental analysis. We also acknowledge Dr Catleya Rojviriya of the Synchrotron Light Research Institute (SLRI) of Thailand for the technical assistance in the XTM testing of samples and the National Research Council of the Philippines (NRCP) for the financial assistance granted to MGY for the manuscript preparation, printing, and binding.

References

1 A. Porras, A. Maranon and I. A. Ashcroft, Characterization of a novel natural cellulose fabric from Manicaria saccifera palm as possible reinforcement of composite materials, *Compos. B Eng.*, 2015, **74**, 66–73, DOI: 10.1016/j.compositesb.2014.12.033.

2 E. J. Vandamme, S. De Baets, A. Vanbaelen, K. Joris and P. De Wulf, Improved production of bacterial cellulose and its application potential, *Polym. Degrad. Stab.*, 1998, **59**, 93–99, DOI: 10.1016/S0141-3910(97)00185-7.

3 A. J. Brown, On an acetic ferment which forms cellulose, *J. Chem. Soc. Trans.*, 1886, **49**, 432, DOI: 10.1039/CT8864900432.

4 A. J. Brown, The chemical action of pure cultivations of *Bacterium aceti*, *J. Chem. Soc. Trans.*, 1886, **49**, 172, DOI: 10.1039/CT8864900172.

5 D. P. Delmer, Cellulose biosynthesis: exciting times for a difficult field of study, *Annu. Rev. Plant Physiol. Plant Mol. Biol.*, 1999, **50**, 245–276, DOI: 10.1146/annurev.arplant.50.1.245.

6 M. Embuscado, J. S. Marks and J. N. Bemiller, Bacterial cellulose II optimization of cellulose production by Acetobacter xylinum through response surface methodology, *Food Hydrocolloids*, 1994, **8**, 419–430, DOI: 10.1016/S0268-005X(09)80085-4.

7 S. Bielecki, A. Krystynowicz, M. Turkiewicz and H. Kalinowska, Bacterial cellulose, in *Biopolymers*, ed. E. J. Vandamme, S. De Baets and A. Steinbuechel, Wiley-VCH, Weinheim, 2002, DOI: DOI: 10.1002/3527600035.bpol5003.

8 W. K. Czaja, D. J. Young, M. Kawecki and R. M. Brown, The future prospects of microbial cellulose in biomedical

applications, *Biomacromolecules*, 2006, **8**, 1–12, DOI: 10.1021/bm060620d.

9 T. Khan, J. K. Park and J.-H. Kwon, Functional biopolymers produced by biochemical technology considering applications in food engineering, *Korean J. Chem. Eng.*, 2007, **24**, 816–826, DOI: 10.1007/s11814-007-0047-1.

10 M. Andresen, L. S. Johansson, B. S. Tanem and P. Stenius, Properties and characterization of hydrophobized microfibrillated cellulose, *Cellulose*, 2006, **13**, 665–677, DOI: 10.1007/s10570-006-9072-1.

11 K. Fijałkowski, A. Zywicka, R. Drozd, A. Niemczyk, A. F. Junka, D. Peitler, *et al.*, Modification of bacterial cellulose through exposure to the rotating magnetic field, *Carbohydr. Polym.*, 2015, **133**, 52–60, DOI: 10.1016/j.carbpol.2015.07.011.

12 N. F. Indriyati, B. W. Nuryadin, Y. Irmawati and Y. Srikandace, Enhanced Hydrophobicity and Elasticity of Bacterial Cellulose Films by Addition of Beeswax, *Macromol. Symp.*, 2020, **391**, 1900174, DOI: 10.1002/masy.201900174.

13 Z. Wan, L. Wang, L. Ma, Y. Sun and X. Yang, Controlled hydrophobic biosurface of bacterial cellulose nanofibers through self-assembly of natural zein protein, *ACS Biomater. Sci. Eng.*, 2017, **3**, 1595–1604, DOI: 10.1021/acsbiomaterials.7b00116.

14 H. Suryanto, M. Muhajir, T. A. Sutrisno, Mudjiono, N. Zakia and U. Yanuhar, The mechanical strength and morphology of bacterial cellulose films: the effect of NaOH concentration, *IOP Conf. Ser.: Mater. Sci. Eng.*, 2019, **515**, 012053, DOI: 10.1088/1757-899X/515/1/012053.

15 W. S. Hummers and R. E. Offeman, Preparation of graphitic oxide, *J. Am. Chem. Soc.*, 1958, **80**, 1339, DOI: 10.1021/ja01539a017.

16 D. Han, L. Yan, W. Chen, W. Li and P. R. Bangal, Cellulose/graphite oxide composite films with improved mechanical properties over a wide range of temperature, *Carbohydr. Polym.*, 2011, **83**, 966–972, DOI: 10.1016/j.carbpol.2010.09.006.

17 P.-P. Zuo, H.-F. Feng, Z.-Z. Xu, L.-F. Zhang, Y. L. Zhang, W. Xia and W.-Q. Zhang, Fabrication of biocompatible and mechanically reinforced graphene oxide-chitosan nanocomposite films, *Chem. Cent. J.*, 2013, **7**, 39, DOI: 10.1186/1752-153x-7-39.

18 O. Shezad, S. Khan, T. Khan and J. K. Park, Physicochemical and mechanical characterization of bacterial cellulose produced with an excellent productivity in static conditions using a simple fed-batch cultivation strategy, *Carbohydr. Polym.*, 2010, **82**, 173–180, DOI: 10.1016/j.carbpol.2010.04.052.

19 A. Mulet, J. A. Carcel, N. Sanjuan and J. Bon, New food drying technologies-use of ultrasound, *Food Sci. Technol. Int.*, 2003, **9**, 215–221, DOI: 10.1177/1082013203034641.

20 J. E. Song, J. Su, A. Loureiro, M. Martins, A. Cavaco-Paulo, H. R. Kim and C. Silva, Ultrasound-assisted swelling of bacterial cellulose, *Eng. Life Sci.*, 2017, **17**, 1108–1117, DOI: 10.1002/elsc.201700085.

21 H. Abral, V. Lawrensius, D. Handayani and E. Sugiarti, Preparation of nano-sized particles from bacterial cellulose using ultrasonication and their characterization, *Carbohydr. Polym.*, 2018, **191**, 161–167, DOI: 10.1016/j.carbpol.2018.03.026.

22 D. J. McClements, Advances in the application of ultrasound in food analysis and processing, *Trends Food Sci. Technol.*, 1996, **6**, 293–299, DOI: 10.1016/S0924-2244(00)89139-6.

23 K. Watanabe, M. Tabuchi, Y. Morinaga and F. Yoshinaga, Structural features and properties of bacterial cellulose produced in agitated culture, *Cellulose*, 1998, **5**, 187–200, DOI: 10.1023/A:1009272904582.

24 J. Guo and J. M. Catchmark, Surface area and porosity of acid hydrolyzed cellulose nanowhiskers and cellulose produced by *Gluconacetobacter xylinus*, *Carbohydr. Polym.*, 2012, **87**, 1026–1037, DOI: 10.1016/j.carbpol.2011.07.060.

25 W. Li, J. Yue and S. Liu, Preparation of nanocrystalline cellulose via ultrasound and its reinforcement capability for poly(vinyl alcohol) composites, *Ultrason. Sonochem.*, 2012, **19**, 479–485, DOI: 10.1016/j.ultsonch.2011.11.007.

26 H.-P. Zhao and X.-Q. Feng, Ultrasonic technique for extracting nanofibers from nature materials, *Appl. Phys. Lett.*, 2007, **90**, 73112, DOI: 10.1063/1.2450666.

27 S. S. Wong, S. Kasapis and D. Huang, Molecular weight and crystallinity alteration of cellulose via prolonged ultrasound fragmentation, *Food Hydrocolloids*, 2012, **26**, 365–369, DOI: 10.1016/j.foodhyd.2011.02.028.

28 V. Hospodarova, E. Singovszka and N. Stevulova, Characterization of cellulosic fibers by FTIR spectroscopy for their further implementation to building materials, *Am. J. Anal. Chem.*, 2018, **9**, 303–310, DOI: 10.4236/ajac.2018.96023.

29 M. Ghorbanali, A. Mohammadi and R. Jalajerdi, Synthesis of magnesium hydroxide nanoparticles and cellulose acetate-$Mg(OH)_2$-MWCNT nanocomposite, *J. Nanostruct.*, 2015, **5**, 175–181, DOI: 10.7508/jns.2015.02.013.

30 J. M. Aguirre, A. Gutiérrez and O. Giraldo, Simple route for the synthesis of copper hydroxy salts, *J. Braz. Chem. Soc.*, 2011, **22**, 546–551, DOI: 10.1590/s0103-50532011000300019.

31 N. Kumar and V. C. Srivastava, Simple synthesis of large graphene oxide sheets via electrochemical method coupled with oxidation process, *ACS Omega*, 2018, **3**, 10233–10242, DOI: 10.1021/acsomega.8b01283.

32 H. Luo, J. Dong, F. Yao, Z. Yang, W. Li, J. Wang, X. Xu, J. Hu and Y. Wan, Layer-by-layer assembled bacterial cellulose/graphene oxide hydrogels with extremely enhanced mechanical properties, *Nano-Micro Lett.*, 2018, **10**, 42, DOI: 10.1007/s40820-018-0195-3.

33 J. Zhu, B. Liu, L. Li, Z. Zeng, W. Zhao, G. Wang and X. Guan, Simple and green babrication of a superhydrophobic surface by one-step immersion for continuous oil/water separation, *J. Phys. Chem.*, 2016, **120**, 5617–5623, DOI: 10.1021/acs.jpca.6b06146.

34 Y. Zeng, X. Zhong, Z. Liu, S. Chen and N. Li, Preparation and enhancement of thermal conductivity of heat transfer oil-based MoS_2 nanofluids, *J. Nanomater.*, 2013, 1–6, DOI: 10.1155/2013/270490.

35 H. Abral, A. Basri, F. Muhammad, Y. Fernando, F. Hafizulhaq, M. Mahardika, E. Sugiartib, S. Sapuanc, R. Ilyas and I. Stephane, A simple method for improving the properties of the sago starch films prepared by using ultrasonication treatment, *Food Hydrocolloids*, 2019, **93**, 276–283, DOI: 10.1016/j.foodhyd.2019.02.012.

36 M. Eriksson, S. M. Notley and L. Wågberg, Cellulose thin films: degree of cellulose ordering and its influence on adhesion, *Biomacromolecules*, 2007, **8**, 912, DOI: 10.1021/bm061164w.

37 E. Kontturi, M. Suchy, P. Penttilä, B. Jean, K. Pirkkalainen, M. Torkkeli and R. Serimaa, Amorphous characteristics of an ultrathin cellulose film, *Biomacromolecules*, 2011, **12**, 770–777, DOI: 10.1021/bm101382q.

38 P. Khanjani, H. Kosonen, M. Ristolainen, P. Virtanen and T. Vuorinen, Interaction of divalent cations with carboxylate group in TEMPO-oxidized microfibrillated cellulose systems, *Cellulose*, 2019, **26**, 4841–4851, DOI: 10.1007/s10570-019-02417-w.

39 H. Dong, J. F. Snyder, K. S. Williams and J. W. Andzelm, Cation-induced hydrogels of cellulose nanofibrils with tunable moduli, *Biomacromolecules*, 2013, **14**, 3338–3345, DOI: 10.1021/bm400993f.

40 G. Eda and M. Chhowalla, Chemically derived graphene oxide: towards large-area thin-film electronics and optoelectronics, *Adv. Mater.*, 2010, **22**, 2392–2415, DOI: 10.1002/adma.200903689.

41 M. Nosonovsky and B. Bhushan, Roughness-induced superhydrophobicity, in *Multiscale dissipative mechanisms and hierarchical surfaces. NanoScience and Technology*, Springer, Berlin, Heidelberg, 2008, pp. 81–113, DOI: DOI: 10.1007/978-3-540-78425-8_6.

42 H. Yano, J. Sugiyama, A. N. Nakagaito, M. Nogi, T. Matsuura, M. Hikita and K. Handa, Optically transparent composites reinforced with networks of bacterial nanofibers, *Adv. Mater.*, 2005, **17**, 153, DOI: 10.1002/adma.200400597.

43 Y. Feng, X. Zhang, Y. Shen, K. Yoshino and W. Feng, A mechanically strong, flexible and conductive film based on bacterial cellulose/graphene nanocomposite, *Carbohydr. Polym.*, 2012, **87**, 644–649, DOI: 10.1016/j.carbpol.2011.08.039.

44 K. Qiu and A. Netravali, Bacterial cellulose-based membrane-like biodegradable composites using cross-linked and noncross-linked polyvinyl alcohol, *J. Mater. Sci.*, 2017, **47**, 6066–6075, DOI: 10.1007/s10853-012-6517-9.

45 C. Subtaweesin, W. Woraharn, S. Taokaew, N. Chiaoprakobkij, A. Sereemaspun and M. Phisalaphong, Characteristics of curcumin-loaded bacterial cellulose films and anticancer properties against malignant melanoma skin cancer cells, *Appl. Sci.*, 2018, **8**, 1188, DOI: 10.3390/app8071188.

46 M. Szymańska-Chargot, J. Cieśla, M. Chylińska, K. Gdula, P. Pieczywek, A. Kozioł, K. Cieślak and A. Zdunek, Effect of ultrasonication on physicochemical properties of apple based nanocellulose-calcium carbonate composites, *Cellulose*, 2018, **25**, 4603–4621, DOI: 10.1007/s10570-018-1900-6.

47 W. Cheng, J. Chen, D. Liu, X. Ye and F. Ke, Impact of ultrasonic treatment on properties of starch film-forming dispersion and the resulting films, *Carbohydr. Polym.*, 2010, **81**, 707–711, DOI: 10.1016/j.carbpol.2010.03.043.

48 Z. Wu, S. Chen, R. Wu, N. Sheng, M. Zhang, P. Ji and H. Wang, Top-down peeling bacterial cellulose to high strength ultrathin films and multifunctional fibers, *Chem. Eng. J.*, 2019, 123527, DOI: 10.1016/j.cej.2019.123527.

49 H. Wang, X. Zhang, Z. Jiang, Z. Yu and Y. Yu, Isolating nanocellulose fibrills from bamboo parenchymal cells with high intensity ultrasonication, *Holzforschung*, 2016, **70**(5), 401–409, DOI: 10.1515/hf-2015-0114.

50 S. Taokaew, M. Phisalaphong and B. M. Z. Newby, Bacterial cellulose: Biosyntheses, modifications, and applications, in *Applied Environmental Materials Science for Sustainability*, ed. T. Kobayashi, IGI Global, 2016, pp. 255–283, DOI: DOI: 10.4018/978-1-5225-1971-3.CH012.

51 W. Lin, C. Lien, H. Yeh, C. Yu and S. Hsu, Bacterial cellulose and bacterial cellulose–chitosan membranes for wound dressing applications, *Carbohydr. Polym.*, 2013, **94**, 603–611, DOI: 10.1016/j.carbpol.2013.01.076.

52 Y. Wan, H. Luo, F. He, H. Liang, Y. Huang and X. Li, Mechanical, moisture absorption, and biodegradation behaviours of bacterial cellulose fibre-reinforced starch biocomposites, *Compos. Sci. Technol.*, 2009, **69**, 1212–1217, DOI: 10.1016/j.compscitech.2009.02.024.

53 Q. Lin, Y. Zheng, L. Ren, J. Wu, H. Wang, J. An and W. Fan, Preparation and characteristic of a sodium alginate/carboxymethylated bacterial cellulose composite with a crosslinking semi-interpenetrating network, *J. Appl. Polym. Sci.*, 2013, **131**(3), 39848, DOI: 10.1002/app.39848.